



**Space-borne gravimetric satellite constellations and ocean tides: aliasing effects**

Journal:	<i>Geophysical Journal International</i>
Manuscript ID:	GJI-09-0310.R2
Manuscript Type:	Research Paper
Date Submitted by the Author:	
Complete List of Authors:	Visser, Pieter; Delft University of Technology, DEOS Sneeuw, Nico; Geodatisches Institut Reubelt, Tilo; Geodatisches Institut Losch, Martin; Alfred Wegener Institute van Dam, Tonie; University of Luxembourg, Faculté de Sciences, de la Technologie et de la Communication
Keywords:	GEODESY and GRAVITY, Satellite geodesy < GEODESY and GRAVITY, Time variable gravity < GEODESY and GRAVITY

view

*Geophys. J. Int.* (????) 1??, 1–17

# Space-borne gravimetric satellite constellations and ocean tides: aliasing effects

P.N.A.M. Visser<sup>1</sup>, N. Sneeuw<sup>2</sup>, T. Reubelt<sup>2</sup>, M. Losch<sup>3</sup> and T. van Dam<sup>4</sup>

<sup>1</sup> Delft Institute of Earth Observation and Space Systems, Kluyverweg 1, 2629 HS, Delft, The Netherlands

<sup>2</sup> Geodätisches Institut, Geschwister-Scholl-Str. 24/D, D-70174 Stuttgart, Germany

<sup>3</sup> Alfred Wegener Institute, Bussestrasse 24, D-27570 Bremerhaven, Germany

<sup>4</sup> University of Luxembourg, Faculty of Sciences, Technology and Communication, 6, rue Richard Coudenhove-Kalergi, L-1359 Luxembourg

Received ?? ?? 2009; in original form ?? ?? 2009

## SUMMARY

Ocean tides redistribute mass at high temporal frequencies. Satellite missions that aim to observe medium to low frequency mass variations need to take into account this rapidly varying mass signal. Correcting for the effects of ocean tides by means of imperfect models might hamper the observation of other temporal gravity field signals of interest. This paper explores different methods for mitigating aliasing errors for the specific example of observing mass variations due to land hydrology, including temporal filtering of time series of gravity solutions, spatial smoothing and the use of satellite constellations. For this purpose, an Earth System Model (ESM) was constructed, which included state-of-the-art time varying components for ocean, atmosphere, solid earth, hydrology, ice-sheets, and ocean tides. Using the ESM, we simulated the retrieval of the hydrologically driven gravity field changes using a number of different satellite constellations.

We find that 1) the ocean tide aliasing strongly depends on the satellite constellation, the choice of orbital parameters and the length of the data span; 2) the aliasing effect manifests itself differently for different geographical regions; 3) the aliasing causes a peculiar striping pattern along the ground track of the satellite orbits; 4) optimizing the choice of orbital parameters of a single GRACE-type tandem can be more effective at reducing the aliasing of ocean tide model errors than flying more tandems. Finally, we corroborate the experiences with GRACE data analysis that appropriate post-processing techniques can significantly improve the quality of the retrieved gravity changes.

**Key words:** aliasing – GRACE – low-low satellite-to-satellite tracking – ocean tides mass changes – repeat orbits – satellite constellation – space-borne gravimetry.

## 1 INTRODUCTION

The CHAMP and GRACE missions have demonstrated the tremendous potential for observing mass changes in the Earth system from space (Reigber et al., 1999; Reigber, et al. 2003; Tapley et al., 2004a; Tapley et al., 2004b). The processing of space-borne gravimetric observations, such as low-low (ll) and high-low (hl) satellite-to-satellite tracking (SST) plus accelerometer observations, has reached a point where the major limitation of the accuracy of resolved temporal gravity field models is no longer caused by sensor errors (e.g. observation noise), but by errors in the modelling of mass changes due to the atmosphere, ocean currents and ocean tides. Errors in ocean tide models are considered as one of the major sources of error in the determination of temporal gravity field models from GRACE data (Knudsen and Andersen, 2002; Seo et al., 2008a). Moreover, the problem is exacerbated by the continuously changing ground track for GRACE, which leads to an in-

homogeneous sampling in time and space of gravity field changes. The inhomogeneous sampling results in an extremely complicated pattern of gravity changes due to aliased ocean tides signals. The ocean tides aliasing problem is addressed in more detail in Section 2. Many post-processing data reduction methods have been documented for mitigating the effect of errors in the so-called de-aliasing products. Common approaches for this are smoothing with a Gaussian filter (Wahr et al., 2004; Tapley et al., 2004b) and a correlated error filter for de-striping (Swenson and Wahr, 2006). However, it was found that the impact of such filters is limited, and also that as a negative side effect the gravity field changes one wants to observe are smoothed.

This paper describes a number of possible methods for mitigating the problem of tidal aliasing. It has been investigated if this problem can be reduced in the data processing stage by filtering and spatial smoothing techniques (Section 3.1 and 3.2), and at the mission design stage, by choosing appropriate orbit parameters

## 2 P.N.A.M. Visser et al.

and satellite constellations (Section 3.3). The methods have been tested by simulation, for which we developed a model of "real-earth" time-varying mass distributions (Section 4.1 of this paper, *cf.* (Dam et al., 2008)). With this model, synthetic gravity field retrievals were generated using several different satellite constellations of GRACE-type satellite tandems (Section 4). This closed-loop simulation system allows the rigorous simulation of satellite orbits in the presence of detailed force models (including gravity field changes due to ocean currents and tides, atmosphere, hydrology and ice), low-low satellite-to-satellite tracking (ll-SST) observations and gravity field retrieval (Dam et al., 2008). In addition, the impact of ocean tide model errors and observation noise was investigated. The simulations for each constellation were run for a period of a full year. We then attempted to extract the gravity field changes due to hydrology from the synthetic gravity field retrievals using different methods for reducing aliasing effects. The accuracy of the retrievals was assessed globally and for two selected regions, one close to the equator (Amazon) and one close to the poles (Greenland) (Section 5). Finally, results are summarized and conclusions are drawn (Section 6).

### 2 THE OCEAN TIDES ALIASING PROBLEM

Investigations based on real GRACE data demonstrate that the aliasing errors introduced by inexact models, which are used for the reduction of time variable mass signals with high frequency content, e.g. due to ocean tides, atmosphere variations and ocean currents, lead to severe distortions in the monthly gravity solutions, see for example (Ray and Luthcke, 2006; Seo et al., 2008a; Seo et al., 2008b; Han et al., 2004; Moore and King, 2008). Analyses have indicated that ocean tide modeling errors are currently the dominant error source, *cf.* Figure 4-1 in (Rummel and Koop, 2008). These analyses also indicated that for example errors in the modeling of atmospheric gravity changes have a much smaller effect.

Although Ray and Luthcke (2006) and Seo et al. (2008a) illustrate that the ocean tide aliasing errors seem to be smaller than the calibrated GRACE gravity field errors (Wahr et al., 2006), they are larger than the pre-launch estimate of the gravity field recovery error based on the GRACE instrument error. For a future mission, it is expected that instrumentation will be even more sophisticated, e.g. inter-satellite tracking by high-precision lasers which might improve the range-rate measurement precision by a factor of 100 (Bender et al., 2003; Nerem et al., 2006). In this case, the limiting factor in extracting a gravity change will most certainly not be the instrument sensitivity, but instead the aliasing of the ocean tide modeling errors. Realization of this fact means that methods for the reduction or removal of the aliasing problems have to be advanced if a significant gain in the determination of the time variable geopotential is to be made by a future satellite mission. The impact of sensor noise will be addressed as well in this paper (Section 5.1.1).

In our investigations of ocean tide aliasing, only repeat orbits will be considered. The motivation for this is to keep the aliasing effects due to time-variable ground tracks as low as possible. Furthermore, the sampling of time variable effects, especially of periodic phenomena, such as the ocean tides, is more systematic. Parke (1987) specified the aliasing periods of ocean tides for satellite altimetry (eq. A.2, Appendix A), where point-wise in-situ observations of the sea surface are available. These formulas can also be incorporated for analyzing how ocean tides alias into temporally varying gravity field solutions (Section 3.1). We note that such an analysis can also be done for a mission like GRACE, which does

not fly in a repeat orbit, as documented in e.g. (Ray and Luthcke, 2006; Han et al., 2004; Seo et al., 2008a; Seo et al., 2008b; Ray and Luthcke, 2006). It has to be noted that repeat orbits can be maintained at very low altitudes with state-of-the-art orbit control systems without loss of observations, as is proven by the GOCE mission (Drinkwater et al., 2007).

The spatio-temporal aliasing of ocean tides is much more complicated and complex than simply considering the temporal aliasing frequencies. A very important issue when considering the aliasing in temporal gravity solutions (e.g. monthly GRACE solutions), is also how the phase of the ocean tide constituents are observed by GRACE at different locations along the ground track. Knudsen (2003) showed that different tidal constituents ( $M_2, S_2, K_1, O_1$ ) display different patterns in terms of phase along the GRACE ground track. Seo et al. (2008a) proved that temporal aliasing also leads to spatial distortions. Another effect described in Han et al. (2004) and Seo et al. (2008a; 2008b) are distortions due to integer multiples of the orbital near-resonance order 15 and corresponding degrees of the same parity, which can be explained by Kaula's orbit resonance formulas (Kaula, 1966). These resonance related distortions contribute to the striping pattern in the GRACE gravity field solutions and are mainly visible for tides with aliasing frequencies smaller than the GRACE solution interval (nominally 30 days).

The aliasing effects discussed above occur predominantly at the predicted aliasing frequencies, although some variability might be anticipated due to the non-repeat orbit of GRACE. These spatial distortions show that aliasing effects of ocean tides are not restricted to the oceans. Mass change estimates over land are affected also (in addition to the spatial leakage that can be attributed to the use of spherical harmonics as basis functions, Appendix B) due to the integrated nature of the ll-SST observations, thus affecting e.g. estimates of gravity changes due to hydrology and ice.

For this study, use has been made of the TPXO6.2 (Egbert and Erofeeva, 2002) and FES2004 (Lyard et al., 2006) tide models, which display relatively large differences in the Arctic region (Fig. 1). Such differences typically result in ll-SST observation residuals that are not confined to the Arctic areas, but are spread out over the entire world (see also Section 5).

It might be argued that aliasing effects of tides with aliasing frequencies less than the time-interval between consecutive gravity field solutions (nominally 30 days for GRACE) might be averaged to some extent. As GRACE data analysis has shown, this is partially correct. However, the remaining gravity field recovery errors due to aliasing are still large (Han et al., 2004; Seo et al., 2008a; Seo et al., 2008b).

### 3 REDUCING THE OCEAN TIDAL ALIASING IN SPACE-BORNE GRAVIMETRY

With perfect models for ocean tides, the temporal aliasing problem in space-borne gravimetry would be significantly reduced. However, tidal models are not perfect and their improvement is the subject of significant ongoing research (Savcenko and Bosch, 2008). With every improvement in our tidal models, it is expected that the tidal aliasing effects will be reduced. Unfortunately, practical considerations require other solutions. Given the availability of already decades of high-precision satellite radar altimeter observations, it will be a major challenge to improve tidal models in the near future to such an extent that the associated gravity field recovery error

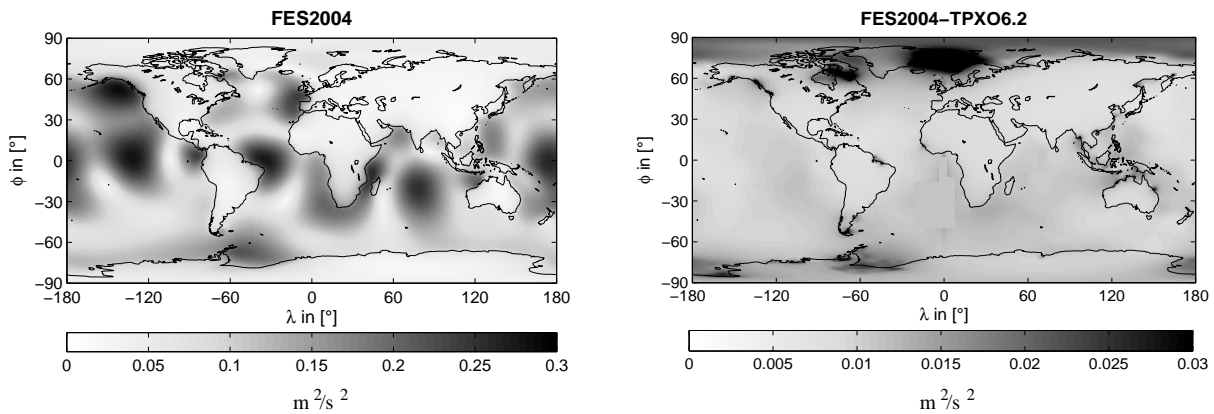


**Figure 1.** Variability of the ocean tidal potential in terms of root-mean-square (RMS) values on a  $1^\circ \times 1^\circ$  grid. Development of the 8 major tidal constituents to maximum SH degree 50: FES2004 model (left) and differences between FES2004 and TPXO6.2 (right).

level is below the recovery error based on the anticipated observation precision for future II-SST ranging systems (see Section 5.1.1).

For new mission designs, the possibility of enhancing and improving data reduction techniques should be taken into account. For example, ocean tides cause perturbations with aliased periods, which can be predicted accurately for repeat orbits. It will be investigated if it is possible to eliminate ocean tide spectral lines from the time series of gravity field spherical harmonic (SH) coefficients (Section 3.1). In addition, it will be attempted to reduce the effect of tidal aliasing by spatial smoothing (Section 3.2). For new mission designs, there is also the obvious trade-off that missions with short repeat periods reduce temporal aliasing at the expense of spatial resolution, and missions with good spatial coverage reduce spatial aliasing at the cost of temporal resolution. To reduce both types of aliasing, more satellites are required. We explore this option in Section 3.3.

### 3.1 Temporal filtering of series of gravity solutions

Ocean tide model errors can have a significant impact on the observation of gravity changes due to hydrology as observed by gravimetric satellites. For such satellites that fly in repeat orbits, it can be anticipated that tide model errors alias at particular frequencies, just as occurs in the observation of sea level by altimeters (Schlax and Chelton, 1994; Parke, 1987). Therefore, it is interesting to investigate if the retrieved gravity field models (spherical harmonic coefficients) can be corrected by estimating the amplitudes for those periods and then reduced afterward. An approach has been implemented where the gravity field retrieval error due to ocean tide model errors is represented by sinusoidal signals with unknown amplitudes. The time series of gravity field coefficients are then represented as:

$$\begin{aligned} \bar{C}_{lm}(t) &= \sum_{ot=1}^{n_{\text{tide}}} \left[ A_{c,lm} \cos\left(\frac{2\pi}{T_{ot}}t\right) + B_{c,lm} \sin\left(\frac{2\pi}{T_{ot}}t\right) \right] \\ \bar{S}_{lm}(t) &= \sum_{ot=1}^{n_{\text{tide}}} \left[ A_{s,lm} \cos\left(\frac{2\pi}{T_{ot}}t\right) + B_{s,lm} \sin\left(\frac{2\pi}{T_{ot}}t\right) \right] \end{aligned} \quad (1)$$

where,  $\bar{C}_{lm}(t)$ ,  $\bar{S}_{lm}(t)$  are the retrieved spherical harmonic coefficients (one set for each retrieval period, e.g. 30 days for GRACE),  $t$  is the time in the middle of the retrieval period, and  $A_{k,lm}$ ,  $B_{k,lm}$  ( $k = c, s$ ) represent the amplitudes for the number of  $n_{\text{tide}}$  selected aliasing periods  $T_{ot}$ . The coefficients  $A_{k,lm}$ ,  $B_{k,lm}$  ( $k = c, s$ ) are estimated by a least-squares fit and subtracted from the original time series of gravity field coefficients. This procedure carries the risk of absorbing part of the signal of interest (e.g. mass changes due to continental hydrology), especially when the ocean tide aliasing periods  $T_{ot}$  coincide or are close to dominant periods in the signal of interest. Also, if the mission duration or time span of observations is shorter than the ocean tide aliasing periods, the separation of gravity changes due to ocean tides from other gravity changes will be hampered.

### 3.2 Spatial smoothing

In the analysis of time series of GRACE gravity solutions, smoothing with a Gaussian filter can be applied to reduce the effect of distortions or stripes (Wahr et al., 2004; Tapley et al., 2004b). In this paper, a comparable but different straightforward approach is adopted, namely spatial smoothing by applying spherical cap averaging operators to the retrieved spherical harmonic gravity field coefficients. Use will be made of the Meissl or Pellinen smoothing operators (Meissl, 1971; Pellinen, 1966). These operators ( $\beta_{l,\psi}$ ) are both a function of the spherical harmonic degree  $l$  and the resolution  $\psi$  (spherical cap radius in degrees ( $^\circ$ )) and are isotropic:

$$\beta_{l,\psi} = \frac{1}{1 - \cos\psi} \frac{1}{2l + 1} [\bar{P}_{l-1}(\cos\psi) - \bar{P}_{l+1}(\cos\psi)] \quad (2)$$

where  $\bar{P}_l$  represents the normalized Legendre polynomial of degree  $l$ . Any smoothing will not only reduce artefacts, but will also damp the gravity field changes one wants to observe.

It has to be noted that it is not claimed that the selected approach for spatial smoothing is optimal. The adopted approach serves however the purpose of showing the possibilities and effects of spatial smoothing. For GRACE, it has been shown that especially the use of non-isotropic filters has great potential (Kusche2007).

4 *P.N.A.M. Visser et al.*

### 3.3 Satellite constellations

The design of a single-satellite or single GRACE-type tandem mission requires scientists and mission designers to make many trade-offs, such as orbital height (e.g. enhanced sensitivity *vs.* higher atmospheric perturbations at lower altitudes) and repeat period (spatial *vs.* temporal sampling). The choice of these orbital parameters will also determine ocean tide aliasing periods (Section 4). For understanding mass variations at all scales, increased spatial and temporal sampling will always be required. Improved spatial and temporal sampling of the mass field can be achieved by using more satellites or satellite tandems. The complications of designing a single-tandem mission are greatly increased and involve many more choices, i.e. the choice of orbital inclinations (all polar, or different inclinations to get a more homogeneous density of ground tracks in latitude), orbital planes (equal or interleaved ground tracks), etc. In effect, the number of possible mission scenarios is infinite. For this investigation, we have only used a limited number of satellite constellations to assess the impact of ocean tide aliasing on different design specifications.

## 4 SIMULATION SETUP AND MISSION SCENARIOS

Gravity field recovery simulation experiments were conducted for several periods and mission scenarios using a comprehensive force modeling theory (Table 1) and using a software infrastructure that was built around the NASA/GSFC GEODYN software package (Pavlis et al., 2006; Visser and Schrama, 2005).

### 4.1 Simulating observations

A realistic Earth System Model (ESM) was developed. The ESM contains 6-hourly mass changes due to the atmosphere, ocean currents, ice, continental hydrology, and the solid earth. Details regarding the ESM can be found in (Dam et al., 2008). Gravity field variations were modeled by connecting these 6-hourly fields piecewise linearly in time for the year 1996. It has to be noted that ocean tides were modeled separately by spherical harmonics with continuously time-varying coefficients (Appendix B). The GEODYN package was then used to simulate satellite orbits and ll-SST observations in the presence of a comprehensive set of force models (Table 1). Simulated gravity field solutions were derived complete to degree and order 50 (capturing the largest part of gravity field variations).

We assumed that the orbit perturbations are derived from GPS ll-SST observations. Therefore, the gravity field recovery will be based on the combination of time series of ll-SST observations and satellite position coordinates. A weighted least-squares estimation method was used where the weights are, in principle, in accordance with the anticipated observation error levels (the impact of different relative weights between ll-SST and orbit coordinates is assessed as well). An observation time interval of 20 s was used. The synthetic gravity field solutions were simulated using the parameters provided in Table 1.

The observations are processed in daily batches, where for each day orbital parameters (start position and velocity for each satellite) are estimated together with spherical harmonic gravity field coefficients. Gravity field solutions are obtained by combining the normal equations for a specified number of consecutive days. Time series are then obtained covering nominally one year using

**Table 1.** Definition of static and temporal gravity field models that form part of the simulated real world.

Dynamic models	
Static gravity field	GGM01S (Tapley et al., 2003), part complete to degree and order 50
Gravity changes	hydrology, atmosphere, oceans, ice and solid-earth: 6-hourly piecewise linear fields (Dam et al., 2008)
Tidal gravity	Wahr solid earth tides; ocean tides: FES2004 (Lyard et al., 2006)
Third body attraction	Sun, Moon, Mercury, Venus, Mars, Jupiter, Saturn, Neptune, according to JPL DE200 ephemeris
Reference frame	
Polar motion	Earth orientation and length of day from IERS EOP 90 C 04 solution
Coordinate system	J2000; precession IAU 1976 (Lieske model); nutation IAU 1980 (Wahr model)
Measurement models	
ll-SST	20-second integrated Doppler
Orbit	Cartesian coordinates with time step of 20 s

a time step of one day. For example, if gravity solutions are produced for 8-day periods, the first solution covers January 1-8, the second January 2-9, the third January 3-10, etc. (*cf.* (Kurtenbach et al., 2009) where a Kalman filter approach is used for deriving daily gravity field changes).

During the estimation process, the observations are fed to the same software system that was used to simulate them. If the real world as outlined in Table 1 would be used again, the observation residuals would become equal to zero and so would be the estimated gravity field coefficients. However, during this estimation process, the hydrological part of the ESM was not included in the force model. In addition, the ocean tide model was replaced by TPX06.2 (Egbert and Erofeeva, 2002). Thus, observation residuals will be caused by the integrated effect of mass variations due to the ESM hydrology (in the following referred to as input hydrology) and FES2004/TPX06.2 ocean tide model differences. The aim was then to recover the gravity changes due to hydrology from these observation residuals.

### 4.2 Mission scenarios

The GRACE mission provides global coverage because of its polar orbit. The polar orbit is a requirement for observing mass variations in the Arctic and the Antarctic. The GRACE satellites fly in non-repeating orbits. These orbits lead to a continuously changing ground track pattern which in turn might lead to a difference in quality of the e.g. monthly gravity solutions in terms of spatial resolution. Furthermore, the polar orbits have a ground track density that increases towards the poles, introducing a latitudinal change in the resolution of the solutions. These effects can be avoided to a large extent by selecting satellite repeat orbits and by combining satellites that fly in orbits with different inclinations as proposed by e.g. Bender et al. (2008).

In this paper, two kinds of satellite constellations to improve the spatio-temporal aliasing have been investigated, namely so-called homogeneous and heterogeneous ground track strategies. In

## Space-borne gravimetric satellite constellations and ocean tides: aliasing effects 5

**Table 2.** Investigated mission scenarios. Each mission scenario consists of a different combination of the satellite tandem types 1 (polar, 8-day repeat), 2 (polar, 5-day repeat) and 3 (non-polar, 23-day repeat). The inter-satellite distance is indicated by  $\delta$ .

Tandem type	$a$ (km)	$i$ (deg)	$\delta$ (deg)	Repeat period		
				days	rev.	
1	6746.3	90.0	1.958	8/7.98	125	SC1
2	6696.4	90.0	1.958	5/4.99	79	BEN1
3	6784.8	117.4	1.958	23/23.17	360	BEN2

## Label of investigated mission scenarios

SC1	1 pair of type 1
SC12	2 pairs of type 1, 4-day interleaved
SC1234	4 pairs of type 1, 2-, 4- and 6-day interleaved
BEN1	1 pair of type 2
BEN12	2 pairs, 1 of type 2 and one of type 3

homogeneous ground track strategies, satellite tandems based on the same repeat orbit are combined (Reubelt et al., 2009). A satellite flying in a  $\beta/\alpha$ -repeat orbit fulfils  $\beta$  revolutions in  $\alpha$  nodal days, where  $\beta$  and  $\alpha$  are relative primes (Appendix A). In principle, the product of spatial and temporal resolution of a repeat orbit can be considered constant for low earth orbiting satellites. This means that the spatial resolution can not be enhanced without deteriorating the temporal resolution and vice-versa. As a consequence, the spatial resolution can only be improved without losing temporal resolution by means of additional satellite tandems flying interleaved ground tracks. The temporal resolution can only be enhanced without deteriorating the spatial resolution by adding satellite tandems. In our investigations, we have tested the improvement of the temporal resolution by means of flying time-shifted satellite tandems with exactly the same ground track.

Polar orbits lead to a ground track density that increases from equator to poles (Fig. 2). This leads to larger errors in the gravity field solutions for low latitudes. This problem can be overcome by heterogeneous ground track designs, where orbits with different inclinations and repeat periods are combined. Heterogeneous ground track designs have originally been proposed by Bender et al. (2008). These designs are able to improve spatial and temporal resolution simultaneously and also the different aliasing frequencies might be helpful for de-aliasing (Dam et al., 2008).

A number of mission scenarios has been investigated (Table 2). The starting point was a mission consisting of one GRACE-type pair of satellites with an intersatellite distance  $\delta$  of about 230 km (also comparable to GRACE). A purely polar orbit was selected to guarantee full global coverage. The satellites fly in a repeat orbit for which the repeat period is 8 nodal days (7.98 solar days) in which the satellites complete 125 orbital revolutions. This mission scenario is labeled SC1. In addition, two other mission scenarios were investigated consisting of 2 and 4 identical pairs of satellites in identical repeat orbits, labeled respectively SC12 and SC1234. The SC12 second pair of satellites travels the exact same ground track but with a delay of 4 days compared to the first pair. The SC1234 second, third and fourth pairs also travel exactly the same ground track, but with delays of 2, 4 and 6 days compared to the first pair. All these mission scenarios carry the characteristic of a confluence of tracks at the polar areas and thus an inhomogeneous data distribution as a function of latitude. Therefore, also

**Table 3.** Aliasing periods (days, unless indicated otherwise) for the 8 major ocean tidal constituents for different mission scenarios.

Constituent	SC1	SC12	SC1234	BEN1	BEN2
$M_2$	19.18	13.66	13.66	13.66	104.93
$S_2$	182.62	182.66	182.66	182.64	66.47
$N_2$	63.10	9.13	9.13	10.98	374.43
$K_2$	> 100 yr	> 100 yr	> 100 yr	> 100 yr	48.73
$K_1$	> 100 yr	> 100 yr	> 100 yr	> 100 yr	97.46
$O_1$	19.18	13.66	13.66	13.66	50.53
$P_1$	182.62	182.62	182.62	182.63	209.01
$Q_1$	63.10	9.13	9.13	10.98	77.33

Bender-type constellation was selected for comparison, consisting of two GRACE-type pairs of satellites with the same inter-satellite distance, labeled BEN12. The two pairs of satellites of this constellation, labeled respectively BEN1 and BEN2, fly in orbits with a repeat period of respectively 5 and 23 days, in which they complete respectively 79 and 360 orbital revolutions. The orbital inclination is equal to respectively 90 and 117.4 deg (see Fig. 2 for the ground track patterns). As a feature, the Bender constellation leads to a more - be it not perfect - homogeneous ground track density as a function of latitude (Visser, 2009). For additional information regarding the input that led to the choice of these mission scenarios, the reader is referred to Reubelt et al. (2009), Bender et al. (2008) and Dam et al. (2008).

The ocean tides aliasing periods for the selected mission scenarios are derived using eq. A.2 (Appendix A). For the polar satellites, the tidal components  $S_2$  and  $P_1$  have alias periods of about half a year (Table 3). These periods will interfere with semi-annual cycles of mass change processes. The tidal components  $K_1$  and  $K_2$  have almost infinite aliasing periods for the polar satellites, so that we can safely assume that these components hardly affect the observation of gravity changes on time scales up to many years and even decades. The inclusion of non-polar satellites (BEN2) leads to significantly different alias periods, with an alias period of about one year for the  $N_2$  component.

## 5 RESULTS

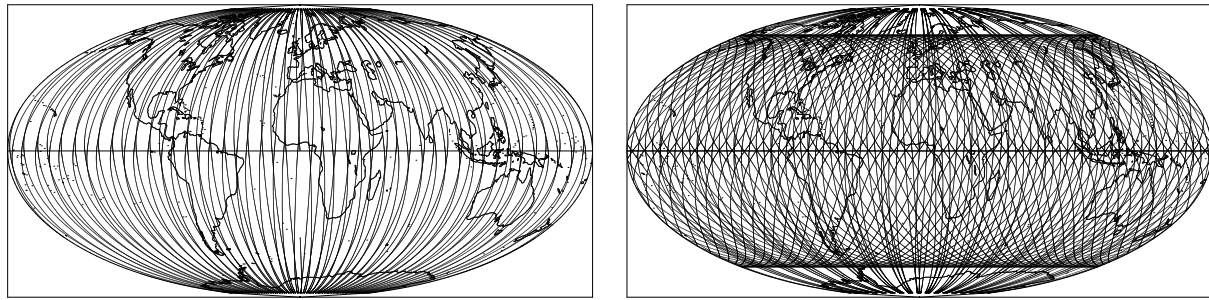
A number of selected gravity field retrieval simulations were conducted, starting with a few bench marks to assess the sensitivity of gravity field retrievals to observation noise and ocean tide model errors, observation weighting, and temporal aliasing (Section 5.1). More extensive simulations were carried out for a period covering a full year (Section 5.2).

For the analysis and the assessment of the different methods and options, we employ Singular Value Decompositions or Empirical Orthogonal Functions (EOFs) of the time series of gravity field solutions on global and regional scales. This technique has been applied successfully to time series of GRACE gravity field solutions for identifying sources of mass change in the earth system, e.g. (Wouters and Schrama, 2007).

### 5.1 Bench marks

#### 5.1.1 Observational noise and ocean tide modeling errors

Initially, use is made of one polar tandem with an 8-day repeat period (SC1). Also, the retrievals were done for one 8-day period

6 *P.N.A.M. Visser et al.*

**Figure 2.** Ground track for SC1 single-tandem polar mission and BEN12 dual-tandem Bender mission for a 2-day period.

(1-8 January 1996), thus combining 8 sets of daily normal equations. The nominal noise level for the Cartesian orbit coordinates is fixed at 1 cm (precision level of orbit determination) and these coordinates are weighted accordingly ( $\sigma_{\text{orbit}} = 1$  cm). The effect of two different II-SST noise levels ( $\sigma_{\text{II-SST}}$ ) has been assessed: 1.0 and 0.01  $\mu\text{m/s}$  by choosing the weight of the II-SST observations accordingly. The 1.0  $\mu\text{m/s}$  is rather conservative considering the GRACE performance (Frommknecht et al., 2006), whereas the 0.01  $\mu\text{m/s}$  is considered feasible with future laser-based sensor systems (TAS, 2008).

Observational noise was added to the error-free observations by using a random Gaussian noise generator with zero mean and standard deviation equal to the above specified noise levels. In addition, by using the FES2004 ocean tide model in the real world and TPX06.2 as reference model when estimating gravity coefficients, we were able to study the effect of the differences between these two ocean tide models.

An observational noise level of 1.0  $\mu\text{m/s}$  leads to larger gravity field retrieval errors than the simulated tide model differences (Fig. 3), but the tide model errors lead to at least an order of magnitude larger gravity field retrieval errors than 0.01  $\mu\text{m/s}$  II-SST observation noise. Based on these results, it can already be concluded that ocean tide model errors need to be reduced significantly when full advantage is to be taken of improved II-SST sensors. Also, ocean tide model errors lead to gravity field retrieval errors larger than the gravity variations due to continental hydrology around spherical harmonic degree 25. However, note that the comparison in terms of spherical harmonics should be considered only as indicative for the true errors and is in fact rather pessimistic, because the gravity changes due to continental hydrology are largely confined to the land areas and the ocean tides to the oceanic regions (although gravity changes are smeared out due to the integrated effect on II-SST observations, see Section 2).

### 5.1.2 Observation weighting

An important issue that needs to be addressed is the weighting of the observations. The nominal standard deviations used for weighting the II-SST ( $\sigma_{\text{II-SST}}$ ) observations and orbit coordinates ( $\sigma_{\text{orbit}}$ ) in the least-squares estimation were taken equal to 1  $\mu\text{m/s}$  and 1 cm, respectively. If the only error source would be Gaussian uncorrelated observation noise, the optimal weights would be commensurate with the observation noise levels. However, when other systematic error sources are introduced, e.g. ocean tide model errors, weighting becomes a complicated issue. It is beyond the scope of this paper to develop a procedure for optimal observation weighting and we refer the reader to previous work in this field, e.g. by Ditmar

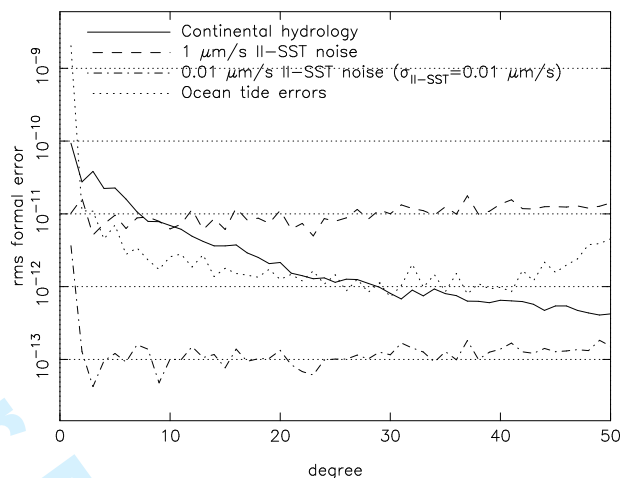


**Figure 3.** Gravity field retrieval error due to different noise levels for 8-day solution with one polar tandem (SC1). An estimate of the gravity field variations due to continental hydrology and gravity field estimation errors due to the differences between the FES2004 and TOP06.2 ocean tide models are included for reference.

et al. (2007). However, one bench mark test has been performed to assess the impact of different weighting in the presence of only ocean tide model errors (thus no observation noise was applied). It was found that the impact on gravity field retrieval error can be significant, particularly at higher spherical harmonic degrees: below degree 30, the impact is marginal (Fig. 4). Even though observation weights may (or are) not optimal for the cases outlined below, it is fair to state that results will be representative of the several possibilities for mitigating the impact of ocean tide model errors that will be explored.

### 5.1.3 Temporal aliasing

Finally, the impact of temporal aliasing was investigated for a few mission scenarios. The bench marks discussed above are based on 8-day retrievals for a satellite flying in an 8-day repeat orbit. Since the gravity field variations due to continental hydrology vary piecewise linearly with 6 hour intervals, temporal aliasing will occur. In addition to the 8-day retrieval for mission scenario SC1, 2-day (January 1-2) and 5-day (January 1-5) retrievals were analyzed for mission scenarios SC1234 and BEN12 (Table 2). As to be expected, the gravity field retrieval error due to temporal aliasing is reduced significantly for shorter sampling intervals (Fig. 5). The retrieval errors due to temporal aliasing are smaller than due to ocean tide model errors (Fig. 4), but larger than due to II-SST

## Space-borne gravimetric satellite constellations and ocean tides: aliasing effects 7

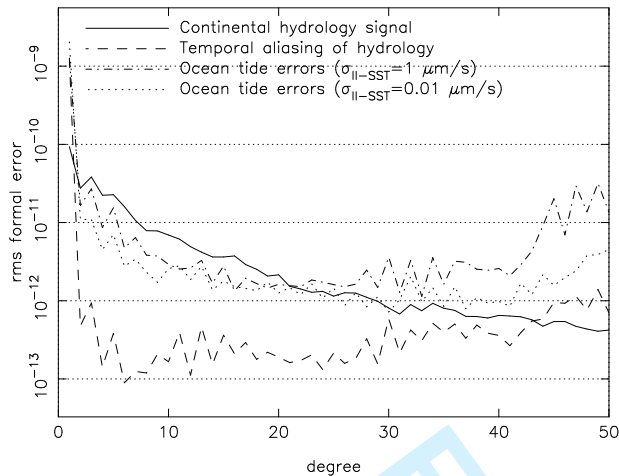


**Figure 4.** Gravity field retrieval error due to TPX06.2 and FES2004 ocean tide model differences for 8-day solution with one polar tandem (SC1) using different II-SST observation weights. An estimate of the gravity field variations due to continental hydrology and gravity field estimation errors due to temporal aliasing are included for reference.

observation noise at a level of  $0.01 \mu\text{m/s}$ . It might thus cautiously be concluded that at some point it is better to invest in constellations of more satellites than in further improvement of II-SST and supporting sensors.

## 5.2 One-year gravity field retrieval simulations

Gravity field retrievals were conducted covering 1996 for several mission scenarios (Section 4.2). Nominally, gravity field retrievals represent periods equal to the repeat period of the orbits that are flown by the (combination of) satellite tandem(s). Thus, for SC1, SC12 and SC1234, solutions were obtained for 8-, 4- and 2-day periods, respectively. All the solutions were obtained with a 1-day time step. For BEN1, time series of 5-day solutions were generated, and for BEN12 both 5-day and 23-day solutions were obtained. It was found that the mass variations due to hydrology can be represented very well by the dominant mode obtained by a Singular Value Decomposition of the time series of associated mass varia-

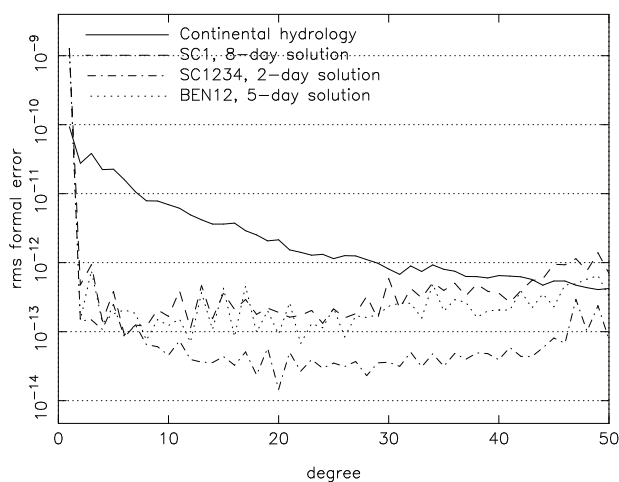


**Figure 5.** Gravity field retrieval error due to temporal aliasing for different retrieval periods and different mission scenarios. An estimate of the gravity field variations due to continental hydrology is included for reference.

**Table 4.** Effect of temporal aliasing and ocean tide model errors on retrieved 1<sup>st</sup> EOFs of continental hydrology for 1996 in terms of global RMS of geoid differences with respect to the truth model.

Filtering	Smoothing (°)	Arc length (day)	Signal (mm)	Error (mm)
one tandem (SC1), temporal aliasing only				
NO	0	8	0.87	0.01
NO	5	8	0.84	0.04
NO	10	8	0.77	0.07
NO	20	8	0.62	0.12
one tandem (SC1), FES2004-TPX06.2				
NO	0	8	0.87	2.00
3 <sup>rd</sup> EOF	0	8	0.87	0.21
NO	5	8	0.84	0.69
NO	10	8	0.77	0.13
NO	20	8	0.62	0.16
one tandem (BEN1), FES2004-TPX06.2				
NO	0	5	0.87	0.12
one tandem (SC1), FES2004-TPX06.2				
YES	0	8	0.87	0.25
YES	5	8	0.84	0.12
YES	10	8	0.77	0.13
YES	20	8	0.62	0.16
two tandems (SC12), FES2004-TPX06.2				
NO	0	4	0.87	0.11
NO	0	8	0.87	0.11
four tandems (SC1234), FES2004-TPX06.2				
NO	0	2	0.88	0.11
NO	0	4	0.87	0.11
NO	0	8	0.87	0.11
Bender two tandems (BEN12), FES2004-TPX06.2				
NO	0	5	0.87	0.11
NO	0	23	0.88	0.61

tions. For example, the first global EOF accounts for 88% of the root-mean-square (RMS) mass variations in terms of global geoid undulations (based on a  $1^\circ \times 1^\circ$  global grid).

### 5.2.1 Nominal gravity field retrievals

In our first retrieval experiment, no error sources were introduced and gravity field changes due to the atmosphere, ocean (currents and tides) and ice were modeled. The use of atmosphere, ocean and ice models at this stage is similar to the atmosphere and ocean dealiasing performed during the retrieval of the GRACE gravity fields (ice is not included in the GRACE dealiasing products). Subsequently, we are left with gravity field variability resulting only from changes in continental hydrology. In this case, any retrieval error would be due to temporal aliasing of the gravity changes due to hydrology alone. We found that the retrieval error was negligible. This fact is also supported by the amplitude of the RMS of the global geoid differences between the first EOF of the input and retrieved gravity field changes (see the first line of Table 4). The RMS of the difference is 0.01 mm. This is very small compared to

8 *P.N.A.M. Visser et al.*

the RMS of the original gravity field changes, 0.87 mm. It has to be noted that temporal aliasing might be reduced to an even lower number by the use of continuous functions in time for the SH gravity field coefficients, but this has not been explored for the research described in this paper.

The effect of the simulated ocean tide model errors on the first EOF of retrieved hydrological gravity changes is displayed in the middle row of Fig. 6 for the case where one polar tandem is used (SC1) and 8-day retrievals are done with a 1-day time step. For reference, the first EOF of the input or true hydrological gravity changes is displayed in the top row of this figure. The original 6-hourly hydrological input models have been averaged to 8-days.

The temporal dependence of the first EOF of the hydrological gravity changes (top row right Fig. 6) displays a clear annual cycle plus a small trend. In contrast, the temporal dependence for the retrieval with the ocean tide model errors resembles the superposition of many periodic signals. The dominant period in the retrieval series is about 63 days, i.e. the aliasing period of the  $N_2$  and  $Q_1$  tides (Table 3). The second EOF for this retrieval also displays such signals (complementing the first EOF, i.e. sine and cosine parts). The third EOF resembles the input hydrological model features, but even this EOF still contains many stripes (Fig. 7). The global RMS of geoid differences is reduced from 2 mm for the first EOF to 0.21 mm for the third EOF (indicated in Table 4).

### 5.2.2 Temporal filtering of series of gravity solutions

For mission scenario SC1, three dominant ocean tides aliasing periods were identified with lengths of 19.18, 182.63 and 63.10 days (Table 3). For these periods, amplitudes were estimated together with a mean for the time series of spherical harmonic coefficients covering 1996. The same time series was corrected afterward by subtracting the estimated sinusoids and mean from the spherical harmonic coefficients. The first EOF for this corrected time series is displayed at the bottom row of Fig. 6. Although stripes can still be observed in the geographical part of the EOF, the time function part contains less variability than the unfiltered case to the extent that the annual signal has become evident. Nonetheless, aliasing remains in the temporal signature as can be observed by comparing the filtered EOF (Bottom Right Fig. 6) with the original input hydrology (top right Fig. 6).

Finally, we note that the striping pattern is strongest close to the equator, i.e. at the latitudes where the biggest distance between adjacent ground tracks exists. The RMS of geoid differences of the first EOF is reduced from 2.0 mm to 0.25 mm, which is comparable to the reduction obtained when using the third EOF (Table 4). The global RMS of geoid corrections for the 1996 time series based on the filtered signal is equal to 1.2, 0.8 and 2.4 mm for the periods of 19.18, 182.63 and 63.10 days, respectively.

### 5.2.3 Spatial smoothing

Spatial smoothing of the first EOF of both the hydrological input model and the gravity field retrievals (filtered and unfiltered) for mission scenario SC1 was applied using Equation 2 for spherical cap radii of  $5^\circ$  and  $10^\circ$  (or about 500 and 1000 km radius). The combination of temporal filtering and  $5^\circ$  spatial smoothing results in a good agreement between the original and recovered hydrological gravity changes for scenario SC1. The RMS of the geoid differences is reduced to 0.12 mm compared to the RMS of the  $5^\circ$  smoothed input hydrology of 0.84 mm (Table 4). Without temporal

filtering, it was found that significant stripes can still be observed around the equator and the RMS is equal to about 0.69 mm. By increasing the spherical cap radius to  $10^\circ$ , a good agreement between original and recovered gravity changes is achieved without temporal filtering (middle Fig. 8). In this case, the RMS of the geoid differences is equal to 0.13 mm compared to a  $10^\circ$  smoothed input hydrology of 0.77 mm. Further increasing the smoothing cap radius results in larger values for the RMS of geoid differences.

### 5.2.4 Different mission scenarios

In addition to the 8-day repeat one polar tandem mission scenario (SC1), a 5-day polar repeat mission was simulated (BEN1). The BEN1 mission results in different aliasing periods as compared with SC1, especially for the  $N_2$  and  $Q_1$  tidal components (about 11 days instead of 63 days, see Table 3). The impact of tide model errors on the first EOF of the retrieved hydrological gravity changes is significantly reduced for this mission scenario. This first EOF compares very well with the first EOF of the input hydrology (Fig. 9). The RMS of geoid differences is reduced from 2.0 to 0.12 mm (Table 4). By reducing the repeat period by flying more tandems, i.e. two (SC12) or four (SC1234), the retrieval can be improved significantly (Fig. 10) and the RMS of geoid differences is reduced from 2.0 to 0.11 mm (Fig. 10). It has to be noted that similar results were obtained for the SC12 4- and 8-day solutions, and the SC1234 2-, 4- and 8-day solutions (Table 4). The 8-day repeat with one polar mission thus appears to be an unfortunate choice when the reduction of ocean tide model errors is a desirable mission goal. For the SC12 and SC1234 mission scenarios, the ocean tides alias periods for  $N_2$  and  $Q_1$  are reduced significantly, from 63.10 to 9.13 days (Table 3). This thus leads to a better averaging out of the associated ocean tides model errors.

The dual-tandem Bender constellation (BEN12) gives a comparable performance as the dual- (SC12) and four-tandem (SC1234) constellations if 5-day solutions are generated (thus using the repeat period of BEN1, top Fig. 11), also in terms of RMS of geoid differences for the first EOF of continental hydrology (Table 4). However, if 23-day solutions are generated (repeat period of BEN2) the results deteriorate significantly. A strong striping pattern can be observed in this case (bottom Fig. 11), and the RMS of geoid differences deteriorates from 0.11 to 0.61 mm (Table 4). Thus, great care has to be taken when defining the data span or time period of the retrievals. Optimizing this data span should be part of the design process for future missions. It can be concluded that improved de-aliasing of ocean tide model errors can be achieved by flying more satellite pairs. However, much can already be gained by tuning orbital parameters (e.g. SC1 vs. BEN1) or by tuning the length of the gravity field retrieval periods (e.g. 5 days vs. 23 days for BEN12).

### 5.2.5 Regional analysis

For many mission scenarios, it can be observed that gravity field retrieval errors depend on the latitude. Relatively large distortions occur at the lower latitudes close to the equator where the distance between adjacent tracks is maximal (e.g. Fig. 6). Therefore, EOF analyses were also conducted for two selected localized areas: the Amazon area close to the equator and the Greenland area close to the Arctic pole. These two areas were selected, because they provide the opportunity of contrasting an annual cycle with a trend, and also a change in ground track density with latitude.

1  
2  
3  
4  
5  
6  
7  
8  
9  
10  
11  
12  
13  
14  
15  
16  
17  
18  
19  
20  
21  
22  
23  
24  
25  
26  
27  
28  
29  
30  
31  
32  
33  
34  
35  
36  
37  
38  
39  
40  
41  
42  
43  
44  
45  
46  
47  
48  
49  
50  
51  
52  
53  
54  
55  
56  
57  
58  
59  
60

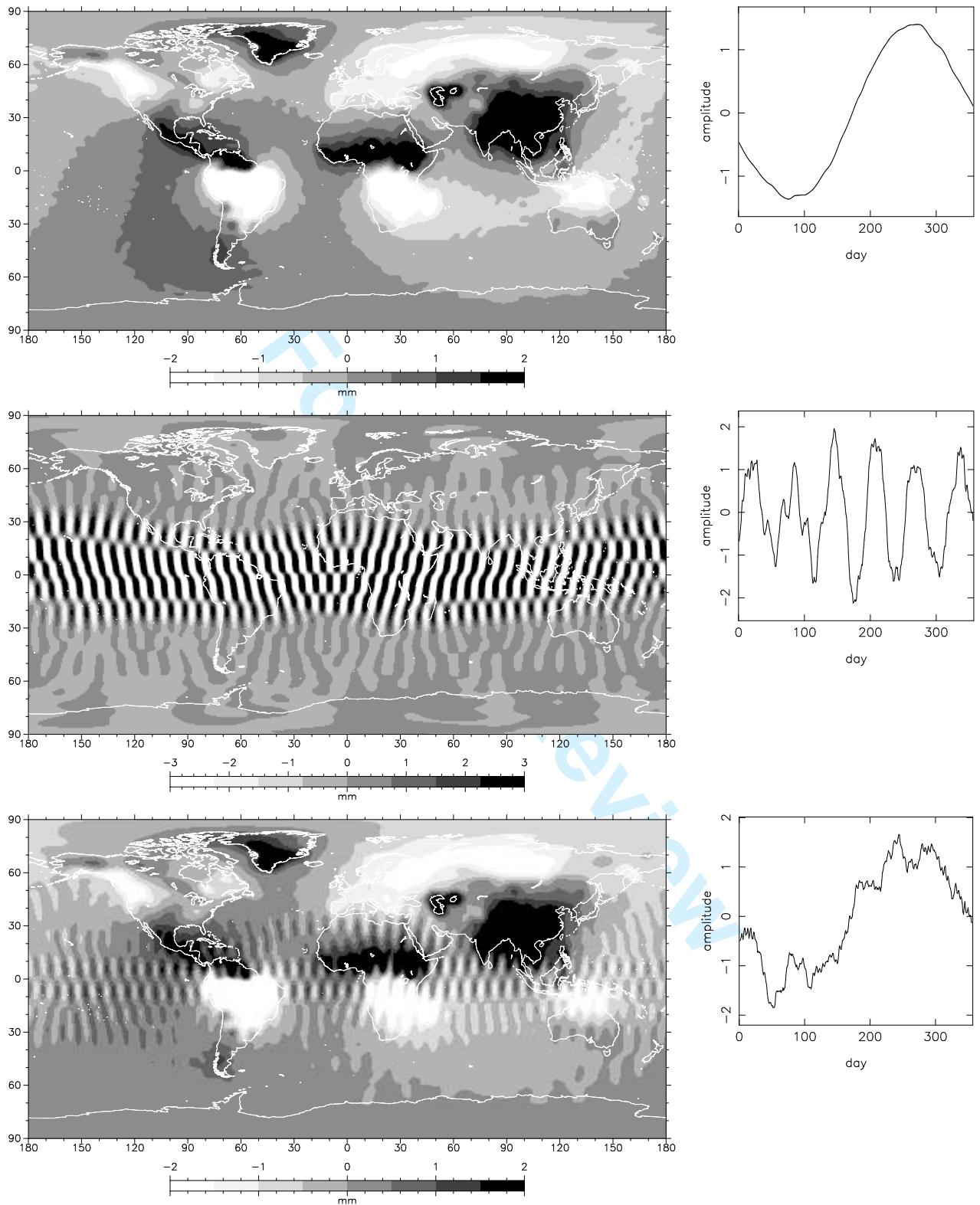


**Figure 6.** First EOF for 1996 continental hydrology: input hydrology (top), full aliasing of ocean tides error (middle) and after filtering out major ocean tides periods (bottom) with one polar tandem (SC1). The EOF is displayed in terms of geoid amplitude (left) and time function (right).

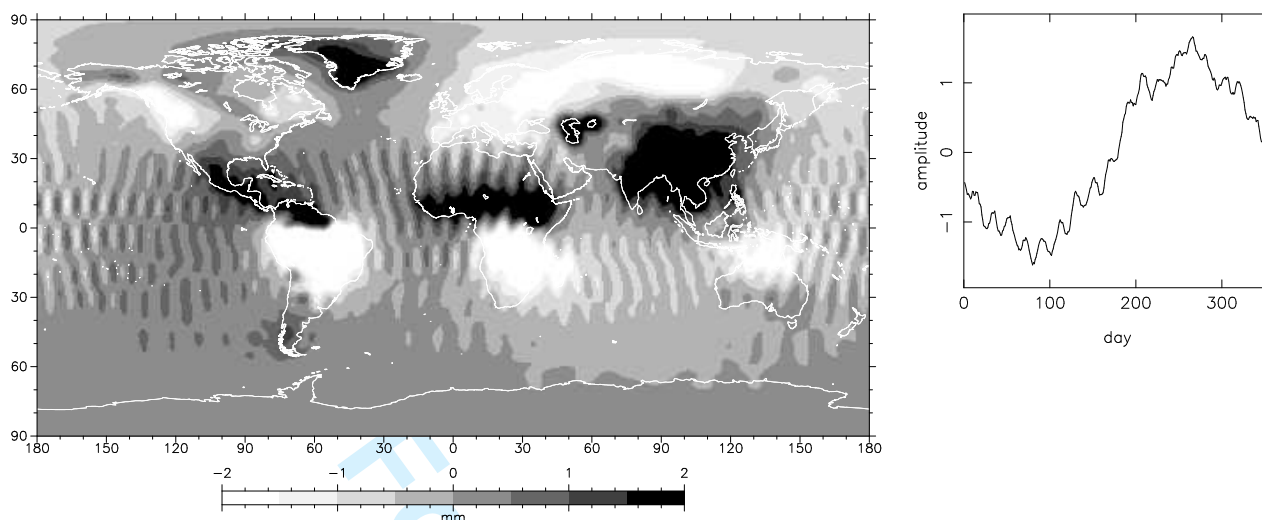


**Figure 7.** Third EOF for 1996 continental hydrology for full aliasing of ocean tides error with one polar tandem (SC1). The EOF is displayed in terms of geoid amplitude (left) and time function (right).

**Table 5.** Comparison between the first EOF of the source and retrieved gravity fields for the Amazon and Greenland area with full aliasing of the ocean tides errors for several mission scenarios. The values are in terms of geoid (mm).

	Unsmoothed		10° spherical cap	
	Signal	Error	Signal	Error
one tandem (SC1), 8-day repeat/solutions				
Amazon	2.42	3.40	2.20	0.09
Greenland	1.21	0.27	1.03	0.14
two tandems (SC12), 4-day repeat/solutions				
Amazon	2.43	0.10	2.20	0.09
Greenland	1.21	0.33	1.03	0.15
four tandems (SC1234), 2-day repeat/solutions				
Amazon	2.43	0.10	2.20	0.10
Greenland	1.21	0.60	1.03	0.28
one tandem (BEN1), 5-day repeat/solutions				
Amazon	2.42	0.10	2.19	0.10
Greenland	1.23	0.28	1.04	0.14
two tandems (BEN12), 5-day solutions				
Amazon	2.42	0.10	2.19	0.08
Greenland	1.23	0.19	1.04	0.10
two tandems (BEN12), 23-day solutions				
Amazon	2.45	0.80	2.22	0.11
Greenland	1.15	0.16	0.97	0.07

The hydrological gravity changes have a clear annual cycle for the Amazon area and a trend for the Greenland area (Fig. 12), indicating the different temporal behavior for these two areas. The aliasing of ocean tide model errors is very prominent for the unsmoothed solutions in the Amazon area, i.e. clear stripes can again be observed in this equatorial region. In contrast, the unsmoothed retrieval for Greenland compares very well with the input hydrology.

In terms of RMS of geoid differences, values of 3.40 and 0.27 mm are found for the Amazon and Greenland regions, respectively, compared to a magnitude of 2.42 and 1.21 mm for the input or true hydrology (Table 5). Thus, for the Amazon area the error of the retrieved gravity changes is larger than the input hydrology, whereas the opposite is the case for the Greenland area.

Smoothing with a 10° spherical cap leads to a first EOF for the Amazon region that compares very well with the input hydrology (right Fig. 12). The RMS of geoid differences is then reduced from 3.40 to 0.09 mm, compared to 2.20 mm for the input hydrology. We conclude that the retrieval results are strongly latitude dependent for the single-tandem 8-day polar repeat mission scenario (SC1). When a 10° spherical cap smoothing is applied, the results for Greenland seem to be worse than for the Amazon region. This might be explained by the fact that the simulated ocean tide model errors are relatively large for the Arctic areas (Fig. 1), thus counteracting the effect of the higher ground track density in case of spherical cap smoothing.

For other mission scenarios, a comparable quality for the first EOF is obtained when applying the 10° spherical cap smoothing (Table 5). However, all other mission scenarios lead to better results for the Amazon area when no smoothing is applied, excluding the 23-day solutions for the Bender constellation, which has a relatively poor quality. It is especially striking that the single-tandem 5-day repeat mission (BEN1) leads to much better results than the 8-day repeat mission (SC1). These results show the complicated interplay between mission scenarios (orbital parameters, number of satellites) and the retrieved gravity changes one wants to observe (trend, annual cycle, geographical location).

## 6 SUMMARY AND CONCLUSIONS

The observation of gravity changes due to continental hydrology has been defined as a test case for assessing the impact of ocean tide model errors. Ocean tide model errors are already considered as a dominant error source for gravity field retrievals from GRACE and with the anticipated technological advance of future sensor systems, these errors will become even more important. A number of (post)processing methods has been investigated, including the tem-

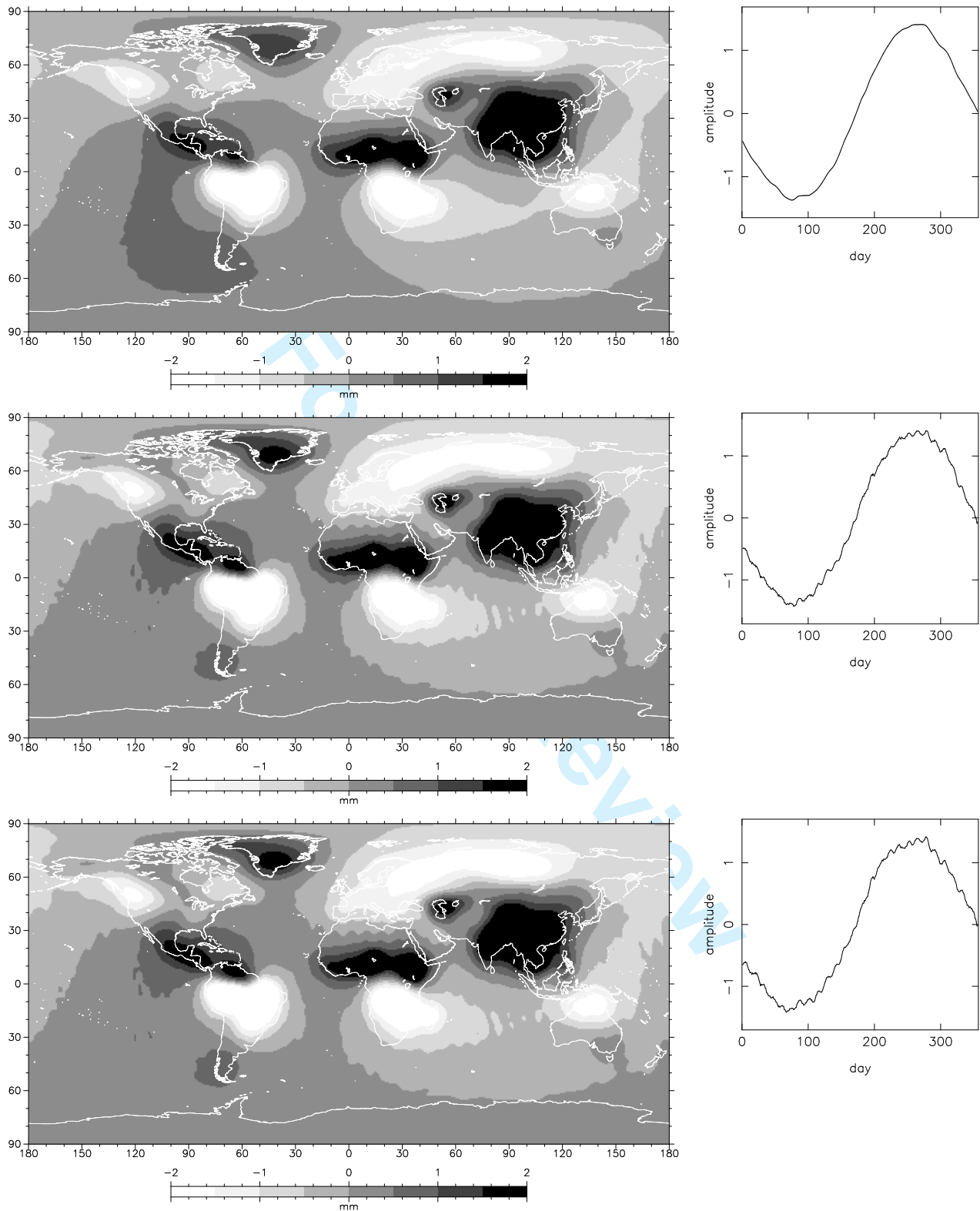


**Figure 8.** First EOF for 1996 continental hydrology applying  $10^\circ$  smoothing: input hydrology (top), full aliasing of ocean tides error (middle) and after filtering out major ocean tides periods (bottom). The EOF is displayed in terms of geoid amplitude (left) and time function (right). The recovery was done with one polar tandem (SC1). The EOF is displayed in terms of geoid amplitude (left) and time function (right).

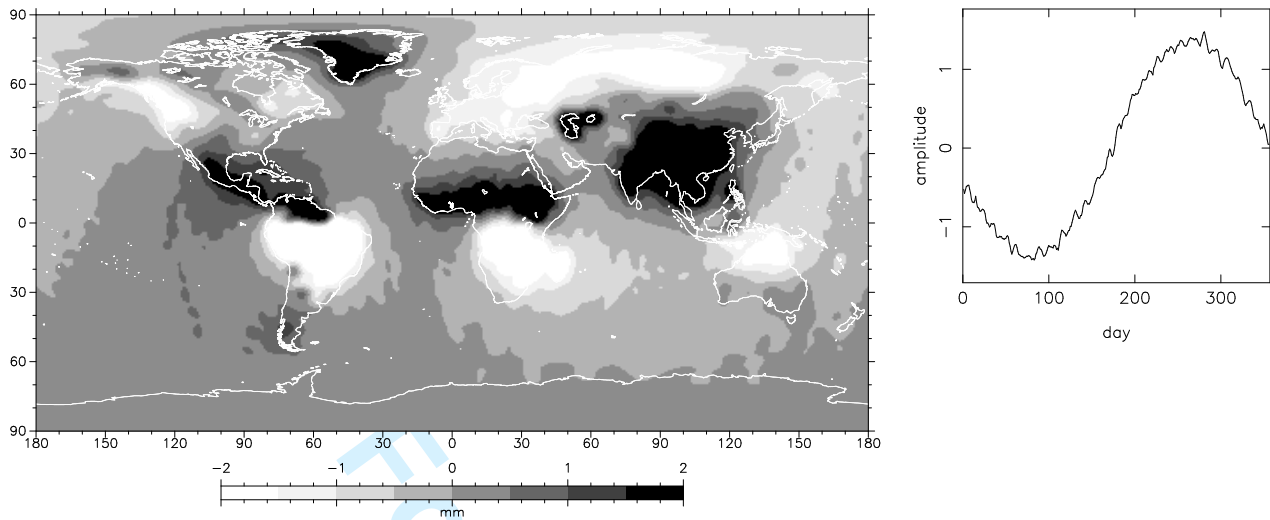


**Figure 9.** First EOF for 1996 continental hydrology with full aliasing of ocean tides error for 5-day repeat polar tandem (BEN1). The EOF is displayed in terms of geoid amplitude (left) and time function (right).

poral filtering of time series of gravity field solutions, the spatial smoothing of these time series and evaluation of solutions for different geographical areas. In addition, the impact of a few selected mission scenarios has been investigated. These mission scenarios include single-tandem GRACE-type missions with different repeat periods, and single-, dual- and four-tandem missions with satellites flying the same repeat period, but interleaved. In addition, a dual-tandem Bender-type mission was defined with satellites flying in orbits with different inclinations. The quality of solutions was in many cases assessed by EOF analysis. The conclusions below are based on this analysis.

First, a few bench mark cases were investigated, showing the need for mitigating the ocean tide model errors if full advantage is to be taken of future sensors with very low noise levels. Also, it was shown that great care has to be taken with the (relative) weights of observed orbit perturbations and II-SST observations. The latter must be taken into account in more detailed follow-on studies.

Second, the effect of ocean tide model errors on the quality of hydrologically driven gravity field retrieval depends strongly on the choice of orbital parameters. For example, a 5-day polar repeat orbit significantly reduced the aliasing of ocean tide model errors compared to an 8-day polar repeat orbit. A strong reduction of this aliasing was also achieved by flying more satellites in identical, but time-shifted orbits. Moreover, the length of the periods for which gravity solutions are generated plays an important role as well. The aliasing of ocean tide model errors is much less for 5-day solutions than for 23-day solutions for the dual-tandem Bender satellite constellation. The RMS of geoid differences for the first EOF of the 1996 hydrological gravity changes could be reduced from 2 mm for the worst case (single tandem, 8-day polar repeat) to 0.12 mm when using different orbital parameters (5-day repeat), to 0.11 mm when using more tandems, and 0.11 vs. 0.61 mm when using 5-day vs. 23-day retrieval periods, where the global RMS of the hydrological gravity changes in terms of geoid is equal to 0.87 mm for the first EOF.

We find that reducing the aliasing of ocean tide model errors can also be achieved by enhancing the (post)processing of time series of gravity field solutions. The ocean tides cause perturbations with alias periods that can be calculated accurately for repeat orbits. Signals with these periods can be filtered out of the gravity

field time series. In principle, the orbital parameters should then be chosen such that these periods do not coincide with the gravity changes one aims to observe. In other words, the ocean tides gravity changes must be separable from - in this case - the hydrological ones. For the worst case mission scenario, the RMS of geoid differences for the first EOF could be reduced from 2 mm to 0.25 mm.

At the expense of reduced spatial detail, spherical cap smoothing was also proven to be successful for identifying hydrological gravity changes in the presence of ocean tide model errors. This was especially the case for the single-tandem polar 8-day repeat orbit, which is obviously far from an optimal mission scenario.

Gravity field retrieval errors display a strong dependency with latitude, which can be explained by the increase of the density of satellite ground tracks with latitude. If, for example, the objective is to observe secular gravity changes in the polar areas, a single satellite tandem already provides a much better sampling in time and space than for observing annual changes in the equatorial areas. A Bender-type constellation consisting of a polar and lower-inclination satellite pair leads to a more homogeneous ground track density as a function of latitude, but then still great care has to be taken with the gravity field retrieval procedure (e.g. 5-day vs. 23-day solutions).

In reality, more error sources will affect gravity changes observed by satellites. These error sources will include not only sensor errors and ocean tide model errors, but also errors in other background models, such as gravity changes due to atmospheric processes and ocean currents. It might be argued that such errors are less systematic than errors in the ocean tide models, but they can significantly impact gravity solutions (Visser and Schrama, 2005; Visser, 2009; Swenson and Wahr, 2006). Taking these error sources into account will further complicate the design of future gravity field missions and (post)processing methodologies and will be part of future research.

Finally, it has to be stated that the results described in this paper are based on a limited number of investigated mission scenarios and therefore the research described in this paper should be considered as indicative and work in progress. The results included in this paper show that the optimization of the design of a future gravity mission is a complicated process. The observation of gravity changes due to hydrology was chosen as test case, but it is fair

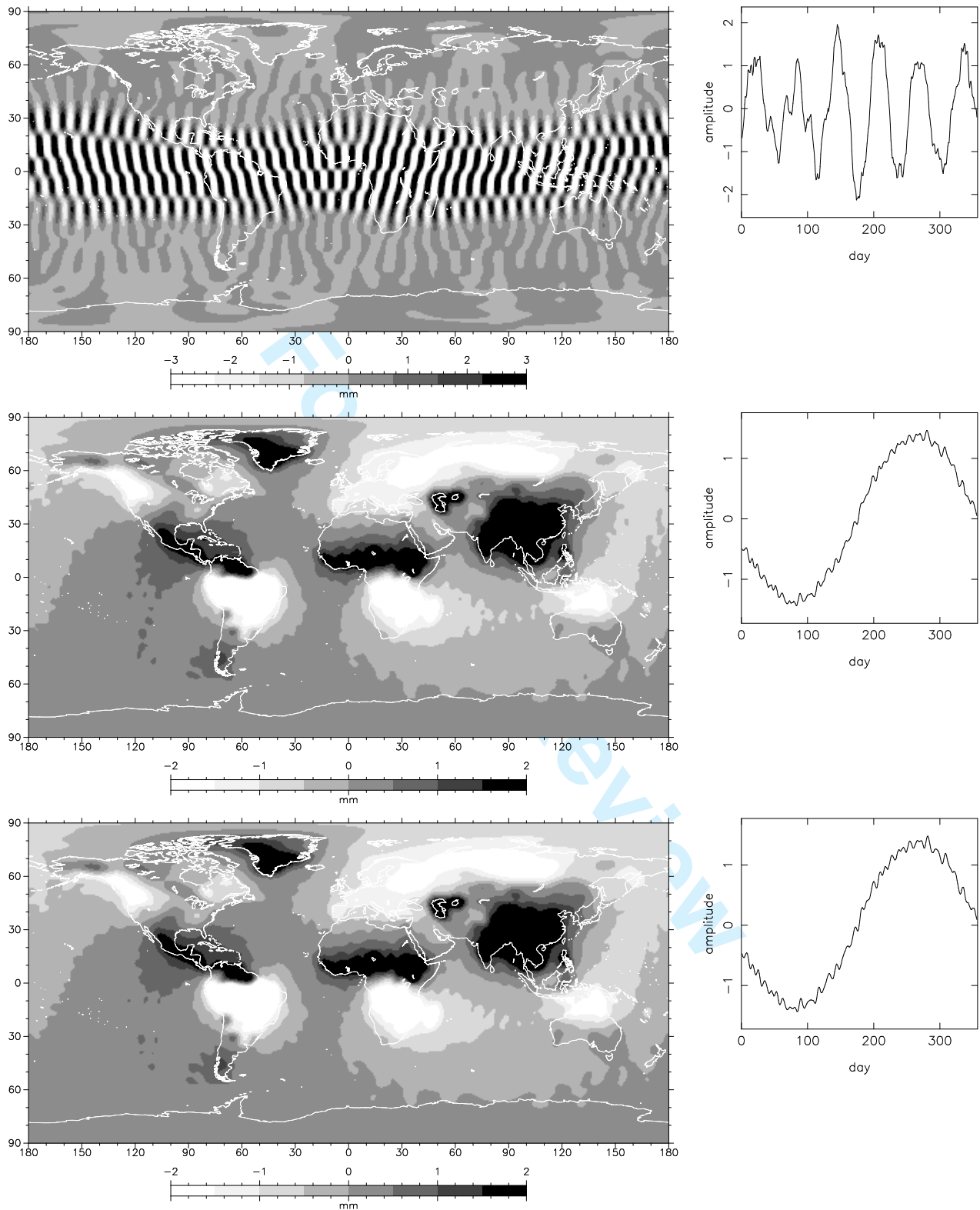


**Figure 10.** First EOF for 1996 continental hydrology with full aliasing of ocean tides error for one (top, 8-day retrievals, SC1), two (middle, 4-day retrievals, SC12) and four (bottom, 2-day retrievals, SC1234) polar tandems in terms of geoid (mm). All polar tandems fly a 8-day repeat. The EOF is displayed in terms of geoid amplitude (left) and time function (right).

1  
2  
3  
4  
5  
6  
7  
8  
9  
10  
11  
12  
13  
14  
15  
16  
17  
18  
19  
20  
21  
22  
23  
24  
25  
26  
27  
28  
29  
30  
31  
32  
33  
34  
35  
36  
37  
38  
39  
40  
41  
42  
43  
44  
45  
46  
47  
48  
49  
50  
51  
52  
53  
54  
55  
56  
57  
58  
59  
60

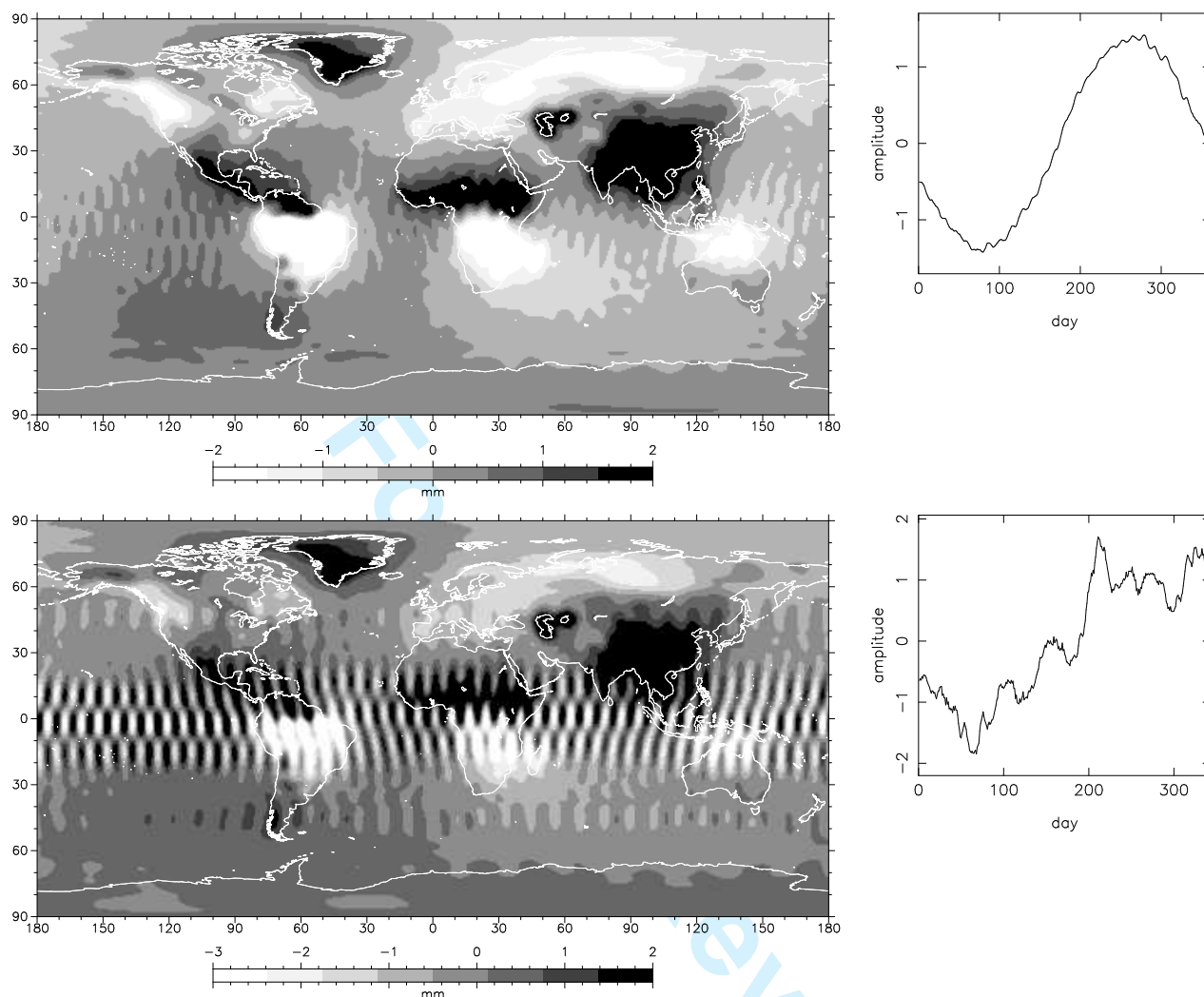


**Figure 11.** First EOF for 1996 continental hydrology with full aliasing of ocean tides error with the two-tandem Bender constellation (BEN12): 5-day (top) and 23-day (bottom) solutions. The EOF is displayed in terms of geoid amplitude (left) and time function (right).

to assume that a future mission will need to be able to do more (e.g. observe ice mass changes as well). This will complicate the mission design even more.

#### ACKNOWLEDGMENTS

The European Space Agency has provided support for the research that led to this paper in the framework of the study *Monitoring and Modelling Individual Sources of Mass Distribution and Transport in the Earth System by Means of Satellites*, ESA Contract 20403. The NASA Goddard Space Flight Center kindly provided the GEO-DYN version 0302.

#### REFERENCES

- Bender, P.L., Hall, J.L., Ye, J. & Klipstein, W.M., 2003. Satellite-satellite laser links for future gravity missions. *Space Sci. Rev.*, 108, 377-384, doi:10.1023/A:1026195913558.
- Bender P.L., Wiese, D.N. & Nerem, R.S., 2008. A possible dual-GRACE mission with 90 degree and 63 degree inclination orbits, *3rd International Symposium on Formation Flying, Missions and Technologies*,

23-25 April 2008, ESA/ESTEC, Noordwijk, The Netherlands, edited by ESA, 1-6.

- Brouwer, D. & Clemence, G.M., 1961. *Methods of Celestial Mechanics*. Academic, New York, 598 pp.
- Dam, T. van, Visser, P., Sneeuw, N., Losch, M., Gruber, T., Bamber, J., Bierkens, M., King, M. & Smit, M., 2008. Monitoring and Modelling Individual Sources of Mass Distribution and Transport in the Earth System by Means of Satellites, *Final Report, ESA Contract 20403*, November 2008.
- Ditmar, P., Klees, R. & Liu, X., 2007. Frequency-dependent data weighting in global gravity field modeling from satellite data contaminated by non-stationary noise, *J. Geodesy*, 81, 81-96.
- Dow, J.M., 1988. Ocean Tides and Tectonic Plate Motions from Lageos. *DGK (Deutsche Geodätische Kommission)*, Reihe C, Nr. 344, Munich.
- Drinkwater, M., Haagmans, R., Muzzi, D., Popescu, A., Floberghagen, R., Kern, M., & Fehring, M., 2007. The GOCE gravity mission: ESA's first core explorer, in *3<sup>rd</sup> GOCE User Workshop, 6-8 November 2006, Frascati, Italy*, pp. 1-7, ESA SP-627.
- Egbert, G.D. & Erofeeva, S.Y., 2002. Efficient inverse modeling of barotropic ocean tides, *J. Atmos. Ocean. Technol.*, 19, 183-204.
- Frommknecht, B., Fackler, U. & Flury, J., 2006. Integrated Sensor Analysis GRACE, *Observation of the Earth System from Space*, 99-113, doi:10.1007/3-540-29522-4-8
- Han, S.C., Jekeli, C. & Shum, C.K., 2004. Time-variable aliasing ef-

## Space-borne gravimetric satellite constellations and ocean tides: aliasing effects 15

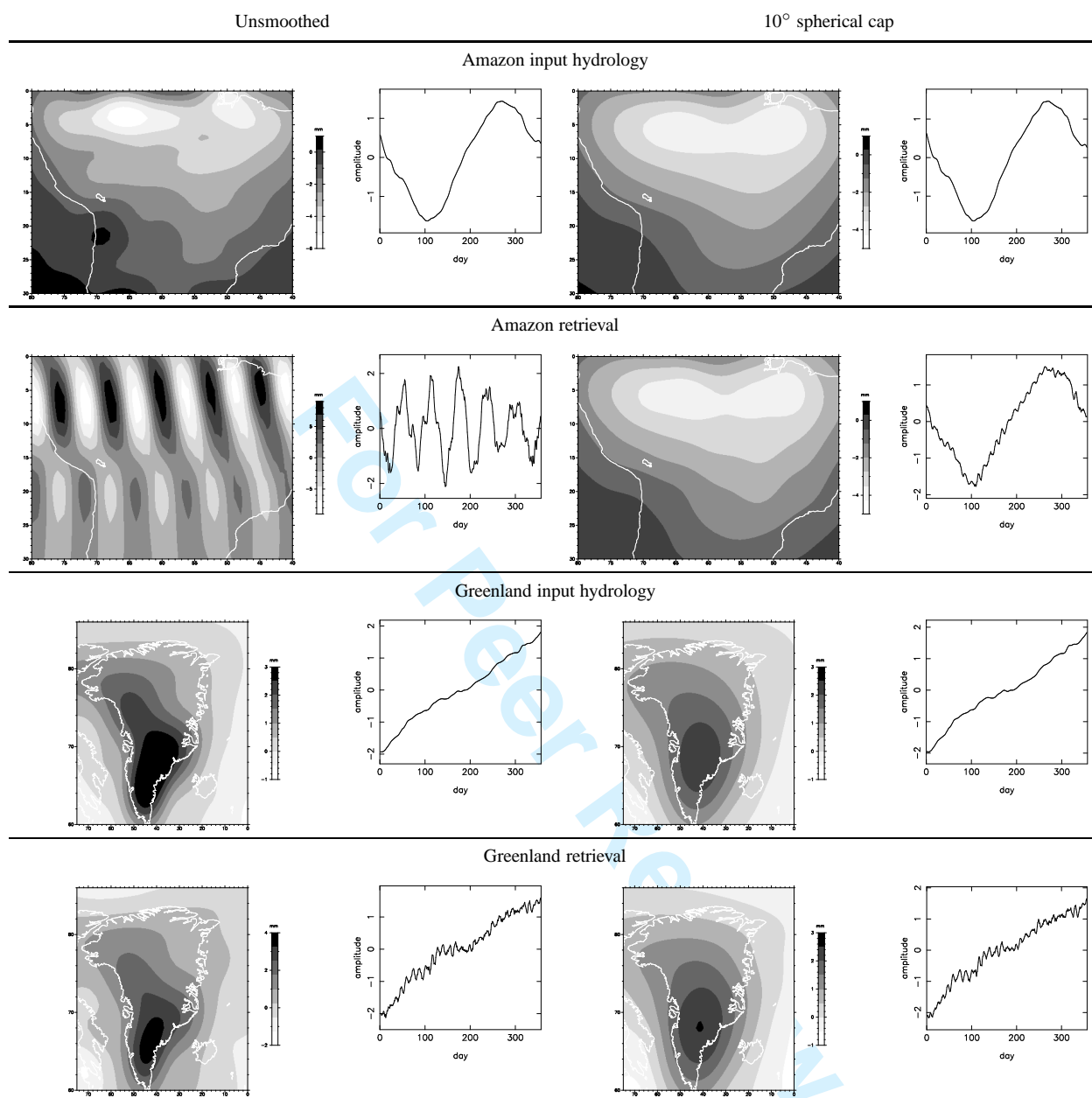


**Figure 12.** First regional EOFs for 1996 continental hydrology with full aliasing of ocean tides error with one polar tandem (SC1) for the Amazon and Greenland areas. The EOFs are displayed in terms of geoid amplitude and time function, unsmoothed (left) and  $10^\circ$  spherical cap smoothed (right).

fects of ocean tides, atmosphere, and continental water mass on monthly mean GRACE gravity field. *J. Geophys. Res.*, 109, B04403, doi:10.1029/2003JB002501.

Kaula, W.M., 1966. Theory of Satellite Geodesy: Applications of Satellites to Geodesy, 120pp., Blaisdell, Waltham, Mass.

King, M.A., Penna, N.T, Clarke, P.J. & King, E.C., 2005. Validation of ocean tide models around Antarctica using on-shore GPS and gravity data. *J. Geophys. Res.*, 110, B08401, doi:08410.01029/02004JB003390.

Knudsen, P. & Andersen, O., 2002. Correcting GRACE gravity fields for ocean tide effects, *Geophys. Res. Lett.*, 29(8), 1178, doi: 10.1029/2001GL014005.

Knudsen, P., 2003. Ocean Tides in GRACE Monthly Averaged Gravity Fields. *Space Sci. Rev.*, 108, 261-270, doi:10.1023/A:1026215124036.

Kurtenbach, E., Mayer-Gür, T. & Eicker, A., 2009. Deriving daily snapshots of the Earth's gravity field from GRACE L1B data using Kalman filter-

ing, *Geophys. Res. Lett.*, 36, L17102, doi:10.1029/2009GL039564.

Kusche, J., 2007. Approximate decorrelation and non-isotropic smoothing of time-variable GRACE-type gravity field models, *J. Geodesy*, 81, 733-749, doi: 10.1007/s00190-007-0143-2.

Lyard, F., Lefevre, F., Letellier, T. & Francis, O., 2006. Modelling the global ocean tides: modern insights from FES2004, *Ocean Dynamics*, 56/5-6, 394-415, doi: 10.1007/s10236-006-0086-x.

Meissl, P., 1971. A Study of Covariance Functions Related to the Earth's Disturbing Potential, Report no. 151, Department of Geodetic Science, OSU, Ohio, Columbus

Moore, P. & King, M.A., 2008. Antarctic ice mass balance estimates from GRACE: Tidal aliasing effects. *J. Geophys. Res.*, 113, F02005, doi:10.1029/2007JF000871.

Nerem, R.S., Bender, P., Loomis, B., Pierce, B., Stephens, M. & Howard, J., 2006. Interferometric range transceiver final report. Instrument Incubator Program, IIP-03-0015, University of Colorado at Boulder and

- Ball Aerospace, Technologies Corp.
- Parke, M.E., Stewart, R.H., Farles, D.L. & Cartwright, D.E., 1987. On the choice of orbits for an altimetric satellite to study ocean circulation and tides. *J. Geophys. Res.*, 92/C11, 11,693-11,707.
- Pavlis, D.E., Poulouise, S. & McCarthy, J.J., 2006. GEODYN Operations Manual, *Contractor report*, SGT Inc., Greenbelt, MD.
- Pellinen L.P., 1966. A method for expanding the gravity potential of the earth in spherical harmonics, *Trans. Cent. Sci. Res. Inst. Geod. Aerial Surv. Cartogr.*, 171, (translated by Aeronautical Chart and Information center, TC-1292, pp. 65-116, 1966, AD 1661810)
- Ray, R.D. & Luthcke, S.B., 2006. Tide model errors and GRACE gravimetry: towards a more realistic assessment. *Geophys. J. Int.*, 167, 1055-1059, doi:10.1111/j.1365-246X.2006.03229.x
- Reigber C., Schwintzer, P. & Lühr, H., 1999. The CHAMP geopotential mission, in *Bollettino di Geofisica Teoretica ed Applicata*, 40/3-4, Sep.-Dec. 1999, Proceedings of the 2nd Joint Meeting of the International Gravity and the International Geoid Commission, Trieste 7-12 Sept. 1998, ISSN 0006-6729, edited by Marson, I., Stünkel, H., 285-289.
- Reigber, C., Schwintzer, P., Neumauer K.H., Barthelmes, F., König, R., Förste, C., Balmino, G., Biancale, R., Lemoine, J.M., Loyer, S., Bruinsma, S., Perosanz, F. & Fayard, T., 2003. Earth Gravity Field Model EIGEN-2, *Adv. Space Res.*, 31/8, 1883-1888.
- Reubelt, T., Sneeuw, N. & Sharifi, M.A., 2009. Future mission design options for spatiotemporal geopotential recovery. *Proceedings of the GGEO (Gravity, Geoid and Earth Observation) Symposium*, June 23-27, 2008, Chania, Crete, Greece, Accepted.
- Rummel, R. & Koop, R., 2008. Report from the Workshop on The Future of Satellite Gravimetry, 12-13 April 2007, ESTEC, Noordwijk, The Netherlands, TUM Institute for Advanced Study, edited by R. Koop and R. Rummel, January 2008.
- Savcenko, R. & Bosch, W., 2008, EOT08a - empirical ocean tide model from multi-mission satellite altimetry, *Report No. 81, Deutsches Geodätisches Forschungsinstitut, München*.
- Schlag, M.G. & Chelton, D.B., 1994. Aliased tidal errors in TOPEX/POSEIDON sea surface height data. *J. Geophys. Res.*, 99 (C12): 24,761-24,775.
- Seo, K.W., Wilson, C.R., Han, S.C. & Waliser, D.E., 2008a, Gravity Recovery and Climate Experiment (GRACE) alias error from ocean tides, *J. Geophys. Res.*, 113/B03405, doi:10.1029/2006JB004747, March 2008.
- Seo, K.W., Wilson, C.R., Chen, J. & Waliser, D.E., 2008b. GRACE's spatial aliasing error. *Geophys. J. Int.* 172, 41-48, doi: 10.1111/j.1365-246X.2007.03611.x
- Smith, A., 1999. Application of Satellite Altimetry for Global Ocean Tide Modeling, *PhD thesis*, Delft University Press, ISBN: 90-407-1933-0
- Swenson, S. & Wahr, J., 2006. Post-processing removal of correlated errors in GRACE data. *Geophys. Res. Lett.*, 33, L08402, doi:10.1029/2005GL025285.
- Tapley, B.D., Chambers, D.P., Bettadpur, S. & Ries, J.C., 2003, Large scale ocean circulation from the GRACE GGM01 geoid, *Geophys. Res. Lett.*, 30/22, 2163, doi: 10.1029/2003GL018622.
- Tapley, B.D., Bettadpur, S., Watkins, M. & Reigber, C., 2004a, The gravity recovery and climate experiment experiment, mission overview and early results, *Geophys. Res. Lett.*, 31, L09607, doi:10.1029/2004GL019920.
- Tapley, B.D., Bettadpur, S., Ries, J.C., Thompson, P.F. & Watkins, M.M., 2004b, GRACE Measurements of Mass Variability in the Earth System, *Science*, 305, 1503-1505.
- Tapley, B., Ries, J., Bettadpur, S., Chambers, D., Cheng, M., Condi, F., G. B. Gunter, Kang, Z., Nagel, P., Pastor, R., Pekker, T., Poole, S. & Wang, F., 2005. GGM02 - An improved Earth gravity model from GRACE. *J. Geodesy*, 79, 467-478, doi:10.1007/s00190-005-0480-z.
- Thales Alenia Space, 2008. Laser Interferometry High Precision Tracking for LEO, *Summary Report*, SD-RP-AI-0584, September 2008.
- Visser, P.N.A.M. & Schrama, E.J.O., 2005, Space-borne gravimetry: how to decouple the different gravity field constituents?, *Gravity, Geoid and Space Missions*, vol. 129 of *International Association of Geodesy Symposia*, edited by C. Jekeli et al., pp. 6-11, Springer-Verlag, Berlin Heidelberg.
- Visser, P.N.A.M., 2009, Designing Earth gravity field missions for the future: a case study, *Proceedings of the GGEO (Gravity, Geoid and Earth Observation) Symposium*, June 23-27, 2008, Chania, Crete, Greece, Accepted.
- Wagner, C., 1991, A Prograde Geosat Exact Repeat Mission, *J. Astron. Sci.*, 39(3), 313-326.
- Wahr, J., Swenson, S., Zlotnicki, V. & Velicogna, I., 2004. Time variable gravity from GRACE: First results. *Geophys. Res. Lett.*, 31, L11501, doi:10.1029/2004GL019779.
- Wahr, J., Swenson, S. & Velicogna, I., 2006. Accuracy of GRACE mass estimates. *Geophys. Res. Lett.*, 33, L06401, doi:10.1029/2005GL025305
- Wouters, B. & Schrama, E.J.O., 2007. Improved accuracy of GRACE gravity solutions through empirical orthogonal function filtering of spherical harmonics, *Geophys. Res. Lett.*, 34, L23711, doi:10.1029/2007GL032098.

## APPENDIX A: REPEAT ORBITS AND TEMPORAL ALIASING OF OCEAN TIDES

A satellite flying in a  $\beta/\alpha$ -repeat orbit completes  $\beta$  revolutions in  $\alpha$  nodal days, where  $\beta$  and  $\alpha$  are relative primes. Thus, the satellite flies over exactly the same geographical location each  $\alpha$  nodal days (the associated period in seconds is indicated by the repeat period  $T_{\text{rep}}$ ). This means that at a fixed geographical location all time-variable effects with frequencies larger than the Nyquist frequency  $f_N = 1/(2T_{\text{rep}})$  will be undersampled and thus alias into frequencies  $f < f_N$ .

The phase difference  $\Delta\phi$  of an harmonic signal with period  $T_s$  between two consecutive passages at a certain geographical location is:

$$\Delta\phi = \frac{2\pi}{T_s} T_{\text{rep}} \quad (\text{A.1})$$

By defining  $\Delta\phi_a = \Delta\phi - 2\pi k$  with  $k$  such that  $\Delta\phi_a \in [-\pi, \pi]$ , the alias period  $T_a$  becomes (Schlag and Chelton, 1994; Parke, 1987; Han et al., 2004):

$$T_a = \frac{2\pi}{\Delta\phi_a} \quad (\text{A.2})$$

The mean semi-major axis  $a$  of the repeat period can be approximated very well by taking into account the secular perturbations caused by the  $J_2$  gravity field term (Brouwer and Clemence, 1961). The length of a nodal day  $T_{\text{nod}}$  then becomes:

$$T_{\text{nod}} = \frac{2\pi}{\omega_e - \dot{\Omega}} \quad (\text{A.3})$$

with  $\omega_e$  the angular velocity of the Earth, and  $\dot{\Omega}$  the rate of change of the right ascension of ascending node of the orbital plane (assuming a circular orbit):

$$\dot{\Omega} = -\frac{3}{2} J_2 \sqrt{\frac{\mu}{a^3}} \left( \frac{a_e}{a} \right)^2 \cos i \quad (\text{A.4})$$

where  $\mu$  represents the Earth's gravity parameter and  $a_e$  the mean equatorial radius. The mean semi-major axis can be derived by using the following equation (Wagner, 1991):

$$a = a_K \left[ 1 - J_2 \left( \frac{R_e}{a_K} \right)^2 \left( 4 \cos^2(I) - \frac{\beta}{\alpha} \cos(I) - 1 \right) \right] \quad (\text{A.5})$$

with  $a_K$  the semi-major axis for a Kepler orbit:

$$a_K = \sqrt[3]{\frac{\alpha^2 GM}{\beta^2 \omega_E^2}} \quad (\text{A.6})$$

which is nothing else than Kepler's third law in repeat-orbit disguise.

**Table B1.** Selected major tidal constituents.

Darwin name	Doodson number	Equilib. amp. (m)	frequency (°/hr)	origin
<i>Semi-diurnal</i>				
$M_2$	255.555	0.2441	28.984	$L$ principal
$S_2$	273.555	0.1138	30.000	$S$ principal
$N_2$	245.655	0.0467	28.440	$L$ major elliptic of $M_2$
$K_2$	275.555	0.0309	30.082	$L/S$ declinational
<i>Diurnal</i>				
$K_1$	165.555	0.1426	15.041	$S$ declinational
$O_1$	145.555	0.1013	13.943	$L$ principal
$P_1$	165.555	0.0473	14.959	$S$ principal
$Q_1$	135.655	0.0194	13.399	$L$ elliptic of $O_1$

$L$ : lunar,  $S$ : solar

## APPENDIX B: OCEAN TIDE MODELING

The 8 major ocean tidal components have been used in this study, including the semi-diurnal terms  $K_2$ ,  $M_2$ ,  $N_2$ ,  $S_2$ , and diurnal terms  $K_1$ ,  $O_1$ ,  $P_1$ ,  $Q_1$  (Table B1, (Smith, 1999)). The original tide models are provided as geographical grids of amplitudes and phases. These grids have been converted to time variable geopotential spherical harmonic expansions  $V_{\text{tid}}^{\text{ocean}}$  complete to degree and order  $L_{\text{max}}$ :

$$V_{\text{tid}}^{\text{ocean}} = \sum_{l=0}^{L_{\text{max}}} \sum_{m=0}^l \left(\frac{a_e}{r}\right)^{l+1} \bar{P}_{lm}(\sin \phi) [c_{lm}^{\text{ocean}}(t) \cos(m\lambda) + s_{lm}^{\text{ocean}}(t) \sin(m\lambda)] \quad (\text{B.1})$$

where  $a_e$  represents the Earth's mean equatorial radius,  $\bar{P}_{lm}$  the normalized Legendre polynomial of degree  $l$  and order  $m$ , and the location is given by the radius  $r$ , geocentric latitude  $\phi$  and longitude  $\lambda$ . The geopotential spherical harmonic ocean tide coefficients  $c_{lm}^{\text{ocean}}$  and  $s_{lm}^{\text{ocean}}$  satisfy:

$$c_{lm}^{\text{ocean}} = 4\pi g a_e \rho_w \frac{1+k_l'}{2l+1} \sum_p [(C_{lmp}^+ + C_{lmp}^-) \cos \theta_p(t) + (S_{lmp}^+ + S_{lmp}^-) \sin \theta_p(t)]$$

$$s_{lm}^{\text{ocean}} = 4\pi g a_e \rho_w \frac{1+k_l'}{2l+1} \sum_p [(S_{lmp}^+ - S_{lmp}^-) \cos \theta_p(t) - (C_{lmp}^+ - C_{lmp}^-) \sin \theta_p(t)] \quad (\text{B.2})$$

where the coefficients  $C_{lmp}^{\pm}$  and  $S_{lmp}^{\pm}$  are related to the prograde (+) and retrograde (-) amplitudes  $\bar{D}_{lmp}^{\pm}$  and phases  $\epsilon_{lmp}^{\pm}$  from the spherical harmonic expansions derived from the original tidal grids  $p = K_1, O_1, P_1, Q_1, K_2, M_2, N_2, S_2$ :

$$C_{lmp}^+ = \bar{D}_{lmp}^+ \cos \epsilon_{lmp}^+; S_{lmp}^+ = \bar{D}_{lmp}^+ \sin \epsilon_{lmp}^+$$

$$C_{lmp}^- = \bar{D}_{lmp}^- \cos \epsilon_{lmp}^-; S_{lmp}^- = \bar{D}_{lmp}^- \sin \epsilon_{lmp}^- \quad (\text{B.3})$$

The density of water is given by  $\rho_w$ , the load number for degree  $l$  by  $1+k_l'$  and the fundamental arguments of the tides by  $\theta_p(t)$ .